Supporting Information for

Melting Point Suppression in new Lanthanoid(III) Ionic Liquids by Trapping of Kinetic Polymorphs: an *In Situ* Synchrotron Powder Diffraction Study

Anthony S. R. Chesman, Mei Yang, Bert Mallick, Tamsyn M. Ross, Ian A. Gass, Glen B. Deacon, Stuart R. Batten,* Anja-Verena Mudring*

General: All materials and solvents were purchased from standard commercial sources and used without further purification. No protective atmosphere was required. Ag(dcnm) was prepared by a literature method.[1] Vibrational spectroscopy was carried out on an Alpha-P ATR-spectrometer from the company Bruker (Karlsruhe, Germany) in attenuated total reflection configuration with a diamond crystal as the internal reflection element. The solid IL was directly pressed on the crystal. Differential scanning calorimetry (DSC) was performed with a computer-controlled Phoenix DSC 204 F1 thermal analyser (Netzsch, Selb, D) with argon as the protection gas. The samples were placed in aluminium pans which were cold-sealed under argon. Experimental data are displayed in such a way that exothermic peaks occur at negative heat flow and endothermic peaks at positive heat flow. DSC runs included heating and subsequent cooling at 5 °C/min. Given temperatures correspond to the onset of the respective thermal process. ^{1}H and ^{13}C NMR spectra were recorded in DMSO-d_6 on a Bruker Advance 400 (9.4 Tesla magnet) with a 5 mm broadband autotunable probe with Z-gradients and BACS 60 tube autosampler. Elemental analyses were performed on a Vario EL elemental analyzer (Elementar Analysensysteme GmbH, Hanau, D). Thermogravimetric analysis was conducted on a Perkin-Elmer Pyris1 instrument under a N_2 atmosphere at a heating rate of 10 °C/min.

A microcrystalline sample of $(N_{4444})_3[Pr(dcnm)_6]$ was loaded into a soda-glass Mark-tube of 0.5mm diameter and sealed with wax. High-resolution synchrotron X-ray powder diffraction studies were carried out using the MYTHEN microstrip detector on the powder diffractometer at BL-10 of the Australian Synchrotron.[2] The samples were housed in 0.5 mm diameter capillaries that were rotated during the measurements. Data were recorded between 273 – 373K in the angular range $5 < 2\theta < 85°$, using X-rays of wavelength 0.77369 Å as estimated using NIST LaB_6 (SRM 660a).

Powder X-ray diffraction (PXRD) measurements of the **Sm** compound were carried out on a Huber G670 diffractometer with image plate detector (MoKα, α = 0.70107nm; Huber, Rimsting, Germany).

Synthesis of $(N_{4444})_3[Ln(dcnm)_6]$ (Ln; Ln = La, Ce, Pr, Nd, Sm): Ag(dcnm) (1.00 g, 4.85 mmol) was added to a solution of $(N_{4444})I$ (915 mg, 2.477 mmol) and $LnCl_3 \cdot 7H_2O$ (0.819 mmol, $LaCl_3 \cdot 7H_2O$ = 304 mg, $CeCl_3 \cdot 7H_2O$ = 305 mg, $PrCl_3 \cdot 6H_2O$ = 291 mg, $NdCl_3 \cdot 6H_2O$ = 294 mg, $SmCl_3 \cdot 6H_2O$ = 299 mg) dissolved in ethanol (20 ml). The solution was covered from light and stirred for one hour, resulting in the formation of a precipitate of AgCl/AgI. The reaction solution was filtered through silica, which was further washed with a sufficient amount of ethanol to remove the yellow product which had adhered to the silica. For the synthesis of **La** the reaction solution was then placed under vacuum to remove the solvent until crystals began to form from the solution. The product was then stored at −50 °C for 42 hours with further crystal growth observed. The yellow crystals were filtered from the reaction solution, immediately washed with cold ethanol and diethyl ether and dried under high vacuum for three hours. Yield: 851 mg, 74 %. ATR-IR (ν_{max}/cm^{-1}): 2961m, 2397w, 2878w, 2227m, 2215sh, 1481m, 1461s, 1400s, 1261m, 1211vs, 1151vw, 1108vw, 1063w, 1035w, 1012w, 886m, 869w, 800w, 784vw/sh, 748vw/sh, 738w, 595 (m), 568m, 481w, 411m. ^{1}H NMR (400 MHz): δ 0.93 (t, 36H, 12(CH_3)), 1.32 (h, 24H, 12(CH_2)), 1.57 (m, 24H, 12(CH_2)), 3.16 (m, 24H, 12(CH_2)); ^{13}C NMR (100.6 MHz): 13.49 (CH_3), 19.22 (CH_2), 23.06 (CH_2), 57.54 (CH_2), 106.69 (–C≡N), 112.88 (–C≡N), 119.08 (C–NO). Anal. Calcd. for $C_{66}H_{108}LaN_{21}O_6$ (1430.61): C, 55.41; H, 7.61; N, 20.56 %. Found: C, 55.66; H, 7.65; N, 21.00 %. For the synthesis of **Ce**, **Pr** and **Nd** the reaction solution was placed under vacuum with heating to remove solvent until only approximately 5 ml of reaction solution remained. The solution was allowed to stand for 18 hours, during which period crystals form. The product was then isolated in the aforementioned fashion. **Ce**: Yield: 685 mg, 59 %. ATR-IR (ν_{max}/cm^{-1}): 2961m, 2937w, 2879w, 2227m, 2215w/sh, 1481m, 1461w, 1398s, 1261m, 1212vs, 1151vw, 1100vw, 1063w, 1035w, 1011w, 963vw, 886m, 869vw, 801w, 783vw/sh, 748sh, 738m, 689vw, 596m, 568m, 481vw, 412m; Anal. Calcd. for $C_{66}H_{108}CeN_{21}O_6$ (1431.82): C, 55.36; H, 7.60; N, 20.54 %. Found: C, 55.37; H, 7.54; N, 21.00 %. **Pr**: Yield: 562 mg, 48 %. ATR-IR (ν_{max}/cm^{-1}): 2961m,

2937w/sh, 2879w, 2227m, 2216w/sh, 1481m, 1461w, 1399s, 1261m, 1211vs, 1152vw, 1108vw, 1064w, 1035w, 1012w, 886m, 869vw, 801w, 748w, 738m, 596m, 568m, 481vw, 411m; Anal. Calcd. for $C_{66}H_{108}N_{21}O_6Pr$ (1432.61): C, 55.33; H, 7.60; N, 20.53 %. Found: C, 55.37; H, 7.64; N, 21.00 %. **Nd**: Yield: 738 mg, 64 %. ATR-IR (ν_{max}/cm^{-1}): 2961m, 2937w, 2878w, 2227m, 2215w/sh, 1481m, 1460w, 1398s, 1261m, 1212vs, 1151vw, 1108vw, 1062w, 1035w, 1011w, 886m, 869vw, 800w, 784vw, 748vw/sh, 738m, 596m, 568m, 481w, 412m; Anal. Calcd. for $C_{66}H_{108}N_{21}NdO_6$ (1435.94): C, 55.20; H, 7.58; N, 20.48 %. Found: C, 55.18; H, 7.32; N, 20.81 %. For the synthesis of **Sm** the reaction solution was placed under vacuum to remove the solvent until only a highly viscous yellow oil remained. This was left to stand at room temperature for several days, after which time crystals formed. The yellow product was then isolated in the aforementioned fashion (552 mg, 47 %). ATR-IR (ν_{max}/cm^{-1}): 2961m, 2937w, 2878w, 2227m, 2216w/sh, 1481m, 1461w, 1398s, 1261m, 1210vs, 1152vw, 1108vw, 1063w, 1034w, 1011w, 886m, 870vw, 801w, 783vw, 738m, 596m, 568m, 412m. Anal. Calcd. for $C_{66}H_{108}N_{21}O_6Sm$ (1442.06): C, 54.97; H, 7.55; N, 20.40 %. Found: C, 55.37; H, 7.58; N, 20.59 %.

Crystallography: A crystal was mounted on fine glass fibre using viscous hydrocarbon oil. Data were collected on either a Bruker X8 Apex II CCD (**Ce**) or a Stoe IPDS I (**Sm**), both equipped with graphite monochromated Mo-Kα radiation (λ = 0.71073 Å). Data collection temperatures were maintained at 123 K except for **Sm**, which was maintained at 170 K using an open flow N_2 cryostream. Integration for **Ce** was carried out by the program SAINT and data was correct for Lorentz-polarization effects and for absorption using the Apex program II Suite[3]. The integration for **Sm** was carried out with the Open VMS program Suite X-Red. Solutions were obtained by direct methods or Patterson synthesis using SHELXS-97[4] followed by successive refinements using full matrix least squares methods against F^2 using SHELXL-97.[4] The program X-Seed was used as a graphical SHELX interface.[5] Hydrogen atoms attached to carbon atoms were placed in idealized positions and refined against a riding model to the atom to which they are attached. CCDC 790887 (**Ce**) and 813884 (**Sm**) contains the crystallographic data for this paper. These data can be obtained free of charge from The Cambridge Crystallographic Data Centre via www.ccdc.cam.ac.uk/data_request/cif.

Crystal Data

$(N_{4444})_3[Ce(dcnm)_6]$ (**Ce**): $C_{66}H_{108}CeN_{21}O_6$, M = 1431.85, red block, 0.30 × 0.30 × 0.20 mm^3, trigonal, space group $R32$ (No. 155), a = b = 17.4269(5), c = 22.3789(6) Å, V = 5885.9(3) Å^3, Z = 3, D_c = 1.212 g/cm^3, F_{000} = 2271, $2\theta_{max}$ = 58.0º, 19769 reflections collected, 3269 unique (R_{int} = 0.0296). Final *GooF* = 0.720, *R1* = 0.0158, *wR2* = 0.0413, *R* indices based on 3263 reflections with I >2σ(I) (refinement on F^2), 146 parameters, 0 restraints. Lp and absorption corrections applied, μ = 0.639 mm^{-1}. Absolute structure parameter = 0.001(6).[6]

$(N_{4444})_3[Sm(dcnm)_6]$ (**Sm**): $C_{66}H_{108}SmN_{21}O_6$, M = 1442.08, yellow block, 0.20 × 0.20 × 0.10 mm^3, trigonal, space group $R32$ (No. 155), a = b = 17.5311(11), c = 22.2630(17) Å, V = 5925.6 (7) Å^3, Z = 3, D_c = 1.212 g/cm^3, F_{000} = 2283, $2\theta_{max}$ = 56.1º, 18914 reflections collected, 6306 unique (R_{int} = 0.1155). Final *GooF* = 1.029, *R1* = 0.029, *wR2* = 0.068, *R* indices based on 3180 reflections with I >2σ(I) (refinement on F^2), 146 parameters, Lp and absorption corrections applied, μ = 0.802 mm^{-1}. Absolute structure parameter = −0.020(11).[6]

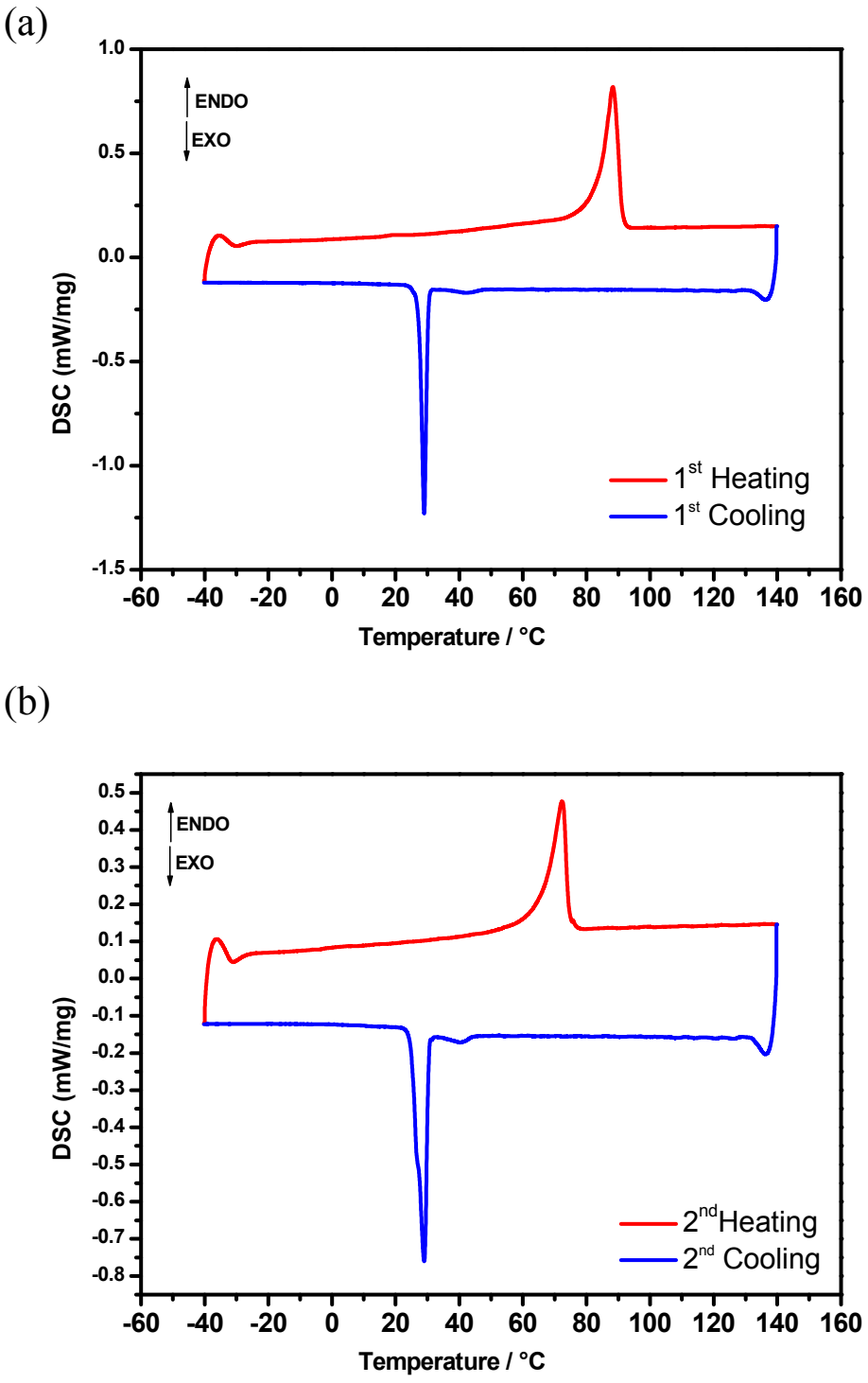

Fig. S1 DSC thermogram of $(N_{4444})_3[La(dcnm)_6]$ (**La**); (a) first heating and cooling cycle; (b) second heating and cooling cycle.

(a)

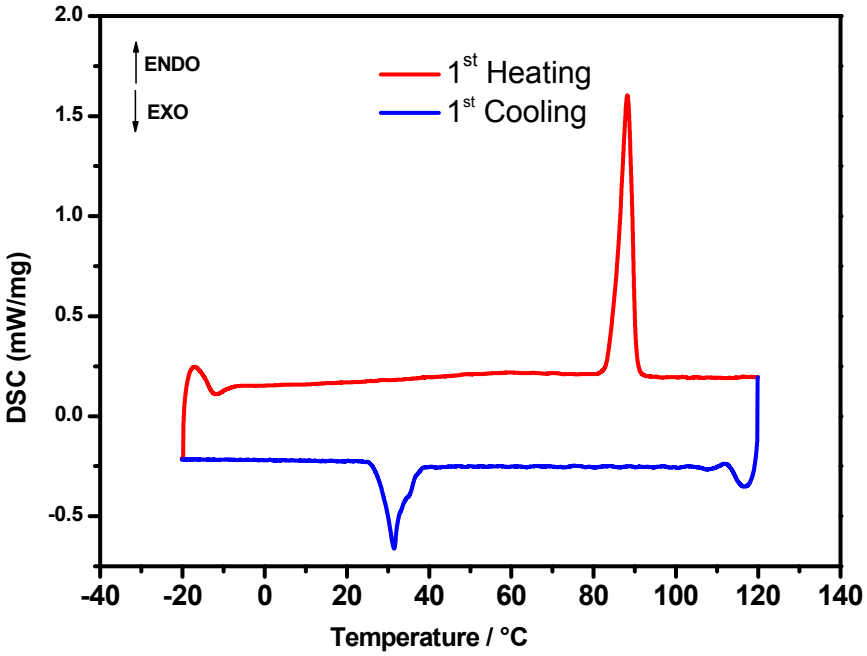

(b)

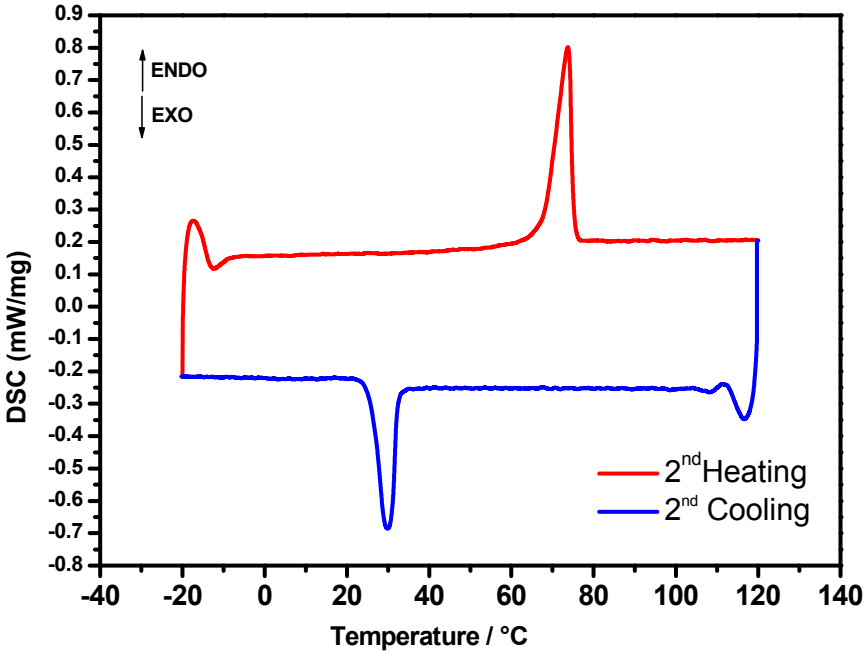

Fig. S2 DSC thermogram of $(N_{4444})_3[Ce(dcnm)_6]$ (**Ce**); (a) first heating and cooling cycle; (b) second heating and cooling cycle.

(a)

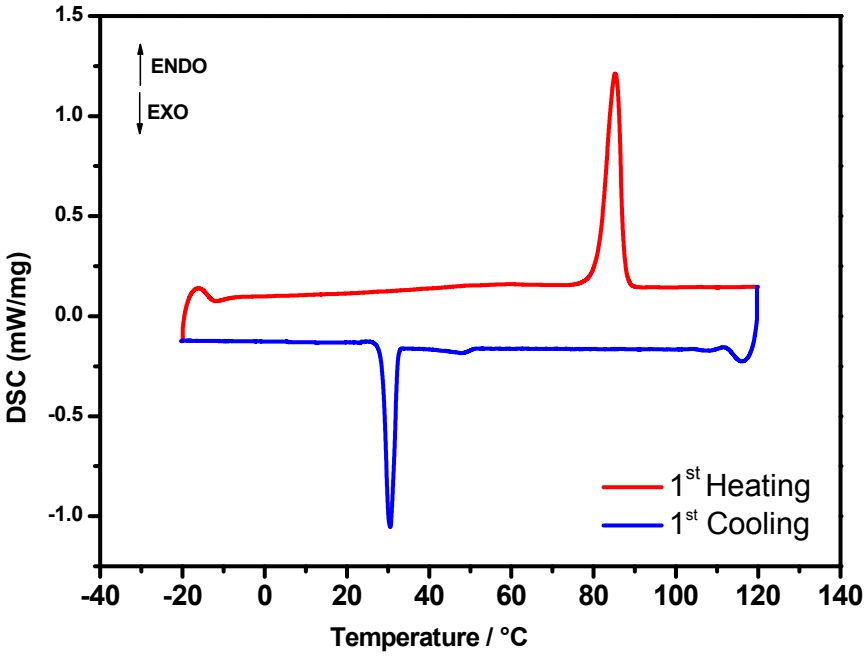

(b)

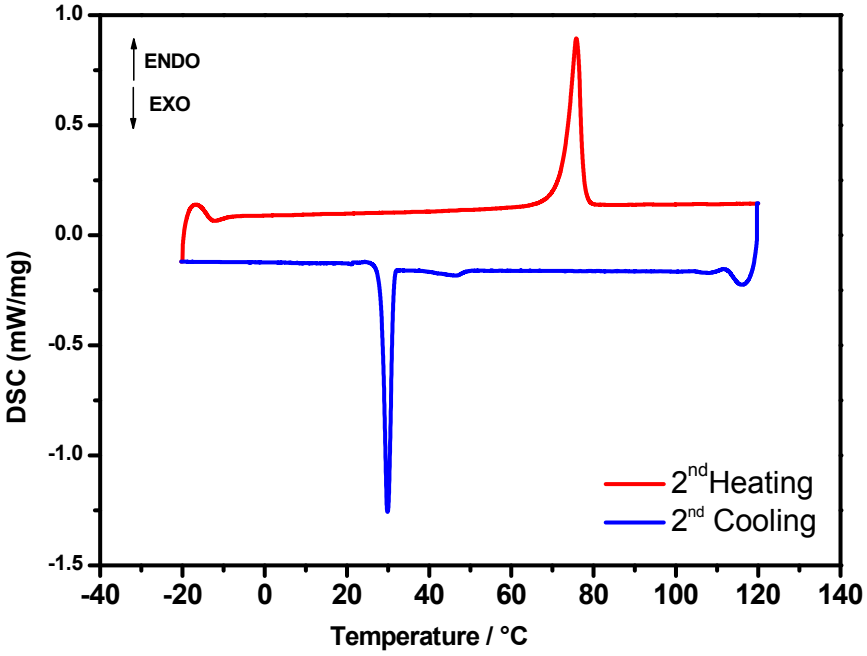

Fig. S3 DSC thermogram of $(N_{4444})_3[Pr(dcnm)_6]$ (**Pr**); (a) first heating and cooling cycle; (b) second heating and cooling cycle.

(a)

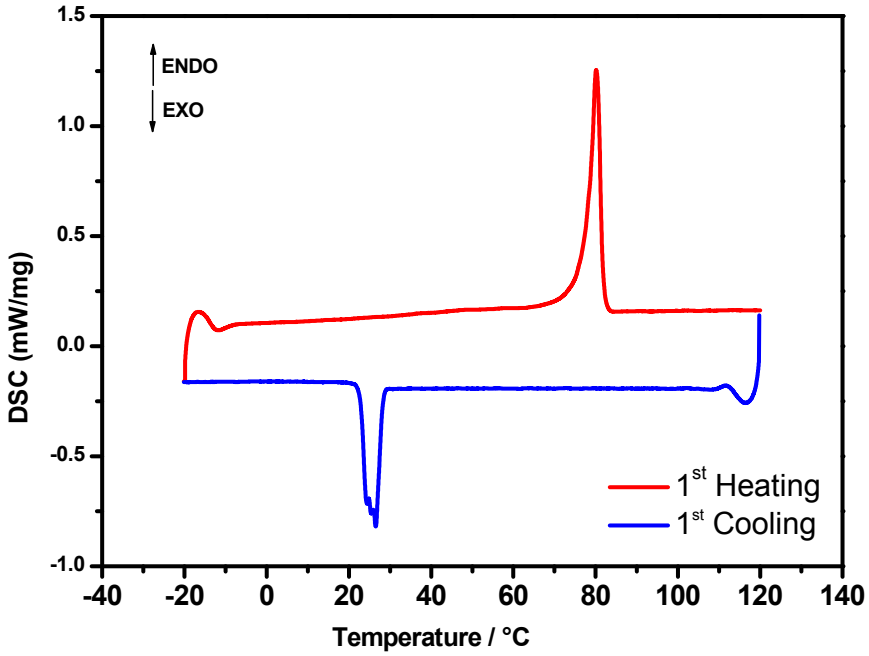

(b)

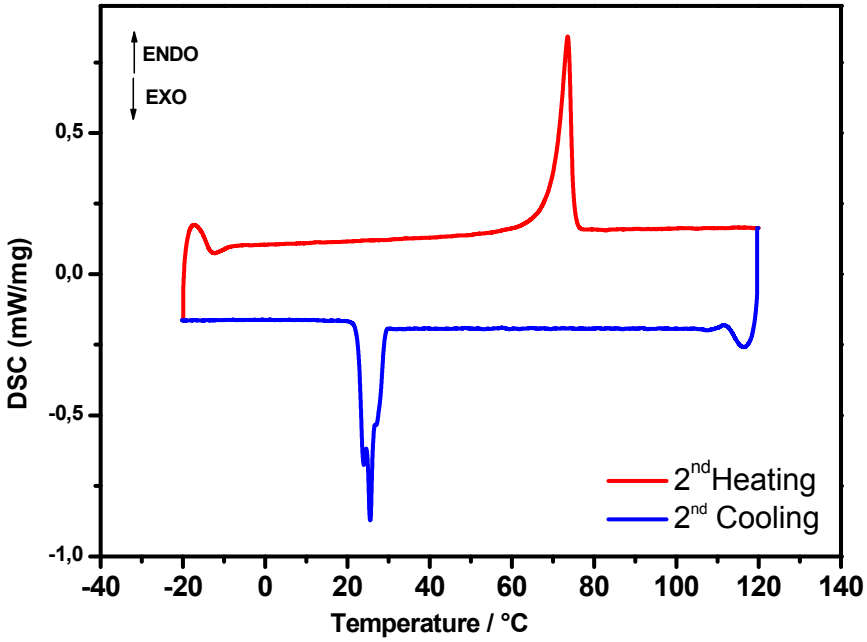

Fig. S4 DSC thermogram of $(N_{4444})_3[Nd(dcnm)_6]$ (**Nd**); (a) first heating and cooling cycle; (b) second heating and cooling cycle.

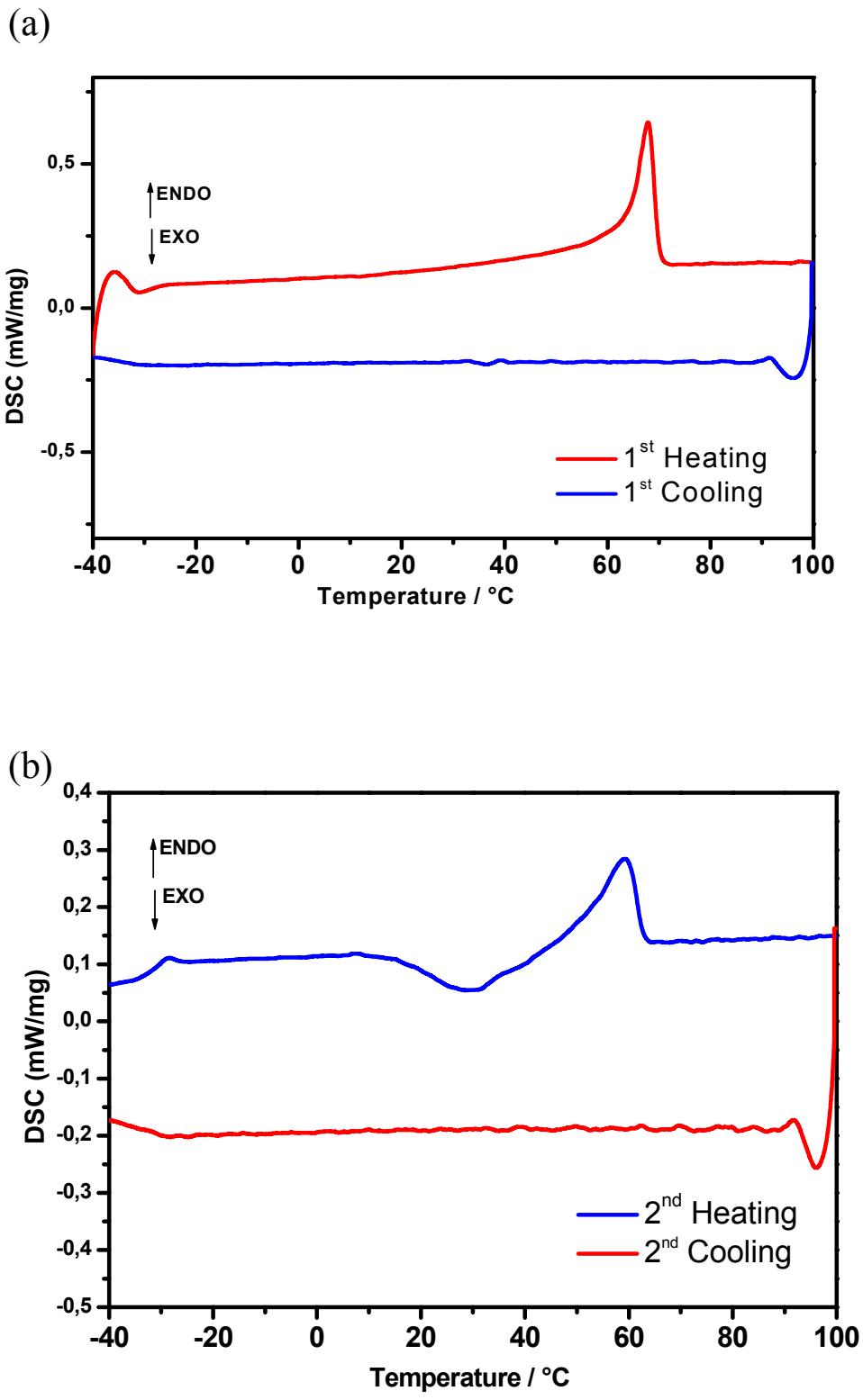

Fig. S5 DSC thermogram of $(N_{4444})_3[Sm(dcnm)_6]$ (**Sm**); (a) first heating and cooling cycle; (b) second heating and cooling cycle.

Table S1 Thermal behaviour of $(N_{4444})_3[Sm(dcnm)_6]$ (**Sm**) as measured by DSC.[a]

	Heating		Cooling	
Cycle	T_t (°C)	ΔH (kJ/mol)	T_t (°C)	ΔH (kJ/mol)
1	57.7 (69.6) [b]	40.8	−30.1 [c]	–
2	−29.9 [b]	–		
	16.9 [d]	−21.0		
	53.0 (60.7) [b]	21.7	−30.1 [c]	–

[a] T_t Temperature of a thermal transition. [b] Melting point. [c] Glass transition. [d] Temperature of recrystallization. Given temperatures mark the onset of a transition, except values in brackets which give the peak maximum for the transition.

For **La** – **Nd** two thermal effects are observed upon cooling, one of less energy content than the other. This might indicate the partial crystallization of the other modification. This would be supported by the fact that in the PXRD of the 2nd heating cycle the strongest reflection for the 1st polymorph is observed together with the reflections of the 2nd polymorph.

The IL $(N_{4444})_3[Sm(dcnm)_6]$ (**Sm**) exhibits thermal behaviour different to the other $(N_{4444})_3[Ln(dcnm)_6]$ ILs. The IL melts upon heating (57.7 °C) but does not recrystallise upon cooling, but rather has a glass transition at −30.1 °C. Upon reheating a glass transition at −29.9 °C is observed and then the IL recrystallises at 16.9 °C. With further heating the IL melts at 53.0 °C. The change in the melting points upon recrystallization indicates that **Sm** also recrystallises as a different polymorph.

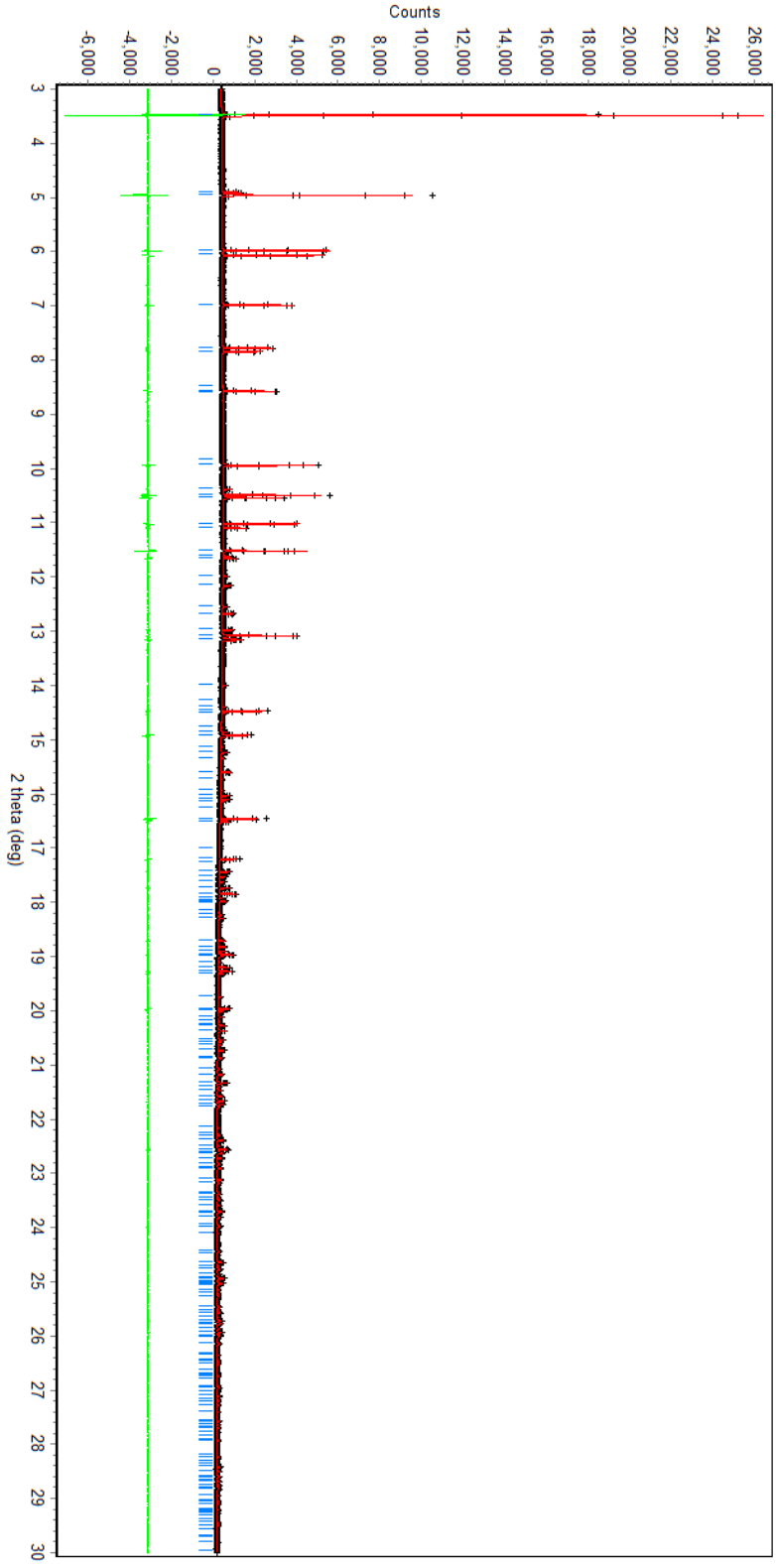

Fig. S6 The refinement of the unit cell parameters of $(N_{4444})_3[Pr(dcnm)_6]$ from the PXRD pattern collected at 273 K using the computer program RIETICA.[7]

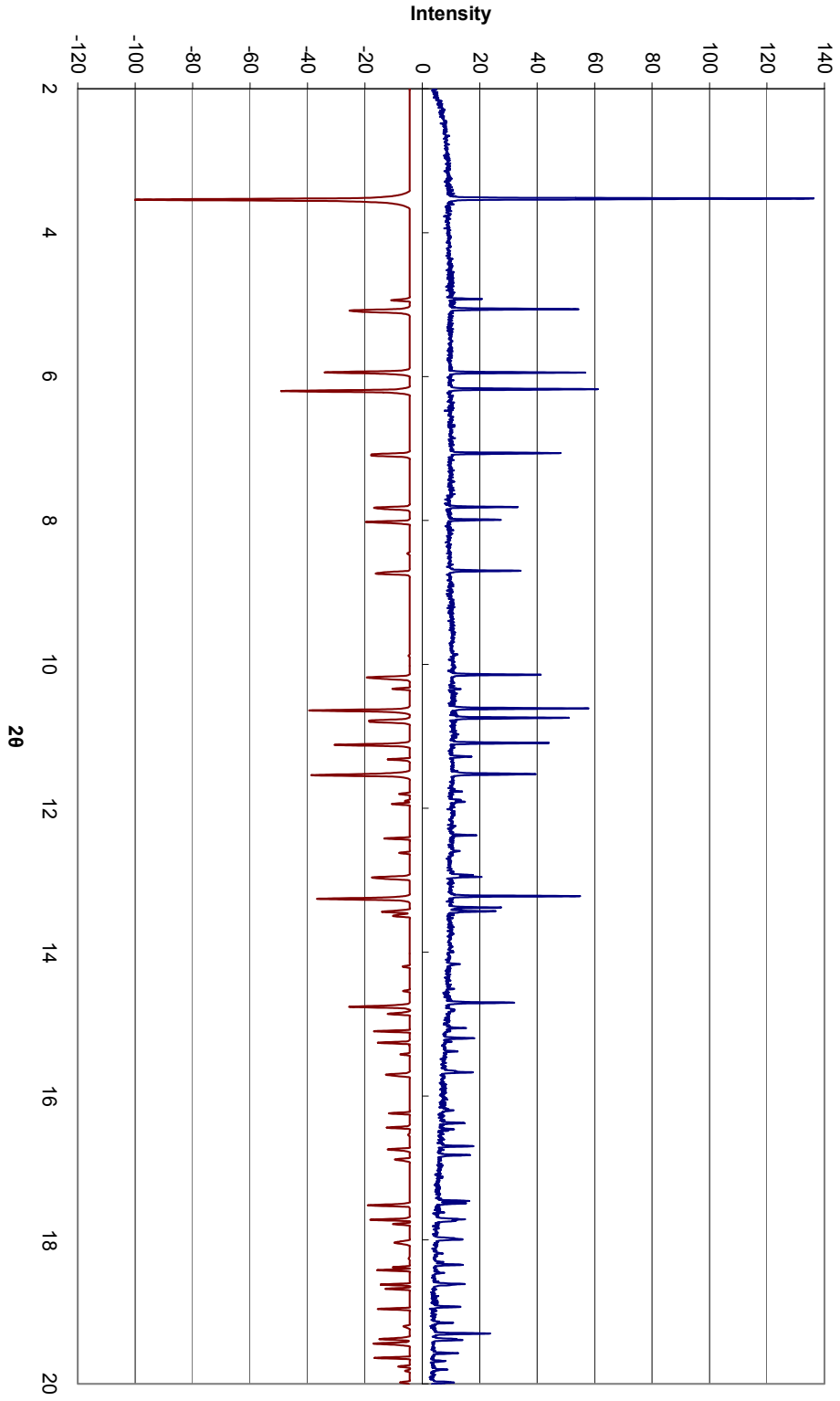

Fig. S7 The X-ray powder diffractogram of $(N_{4444})_3[Pr(dcnm)_6]$ collected at the Australian Synchrotron at 123 K compared to the X-ray powder diffractogram calculated from the SXRD of $(N_{4444})_3[Ce(dcnm)_6]$. Calculated powder pattern was generated using the Mercury v. 1.4.1 software package.[8]

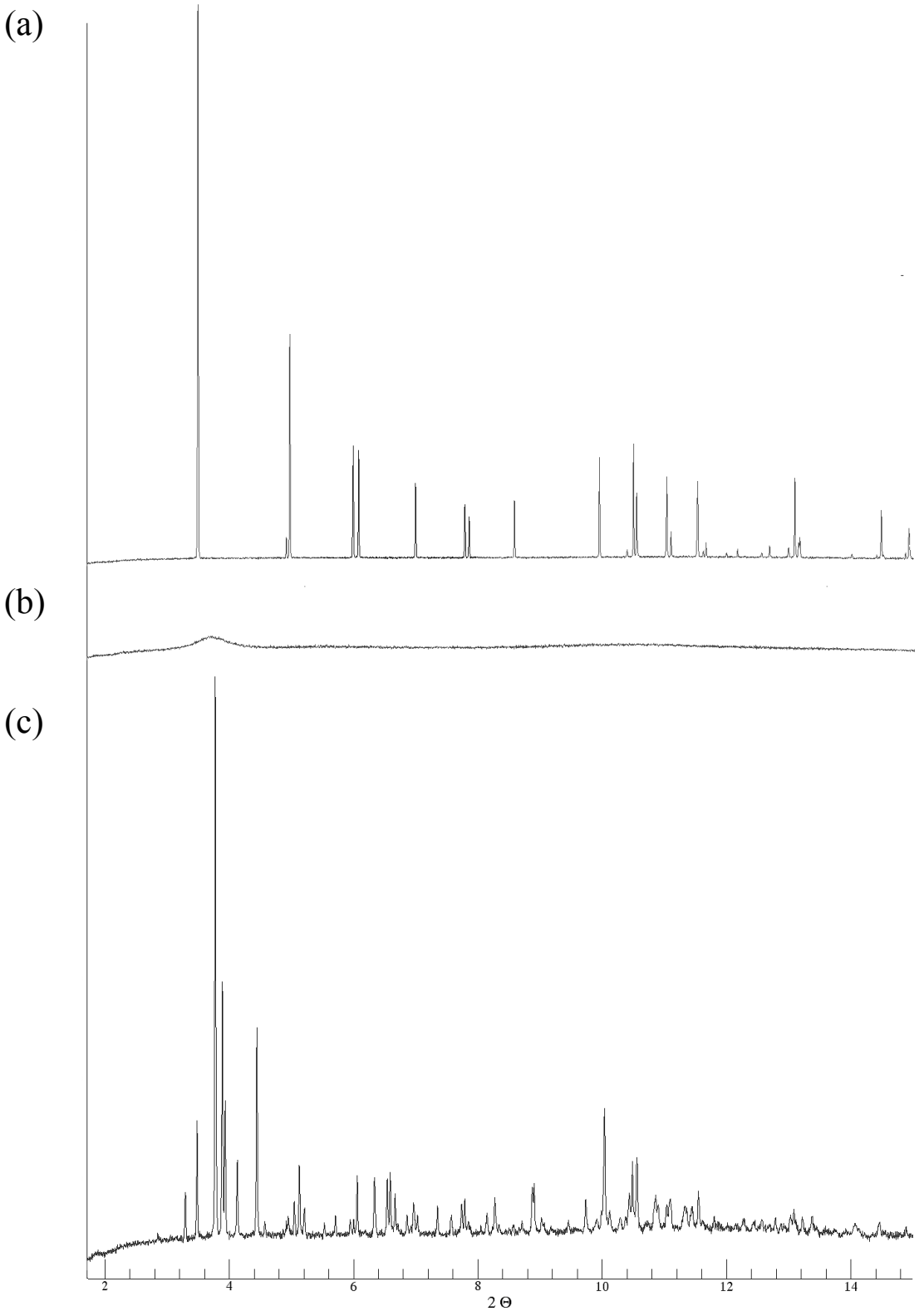

Fig. S8 The X-ray powder diffractograms of (a) the initial polymorph of $(N_{4444})_3[Pr(dcnm)_6]$; (b) the amorphous liquid phase of $(N_{4444})_3[Pr(dcnm)_6]$ and (c) the alternate polymorph of $(N_{4444})_3[Pr(dcnm)_6]$ upon recrystallization.

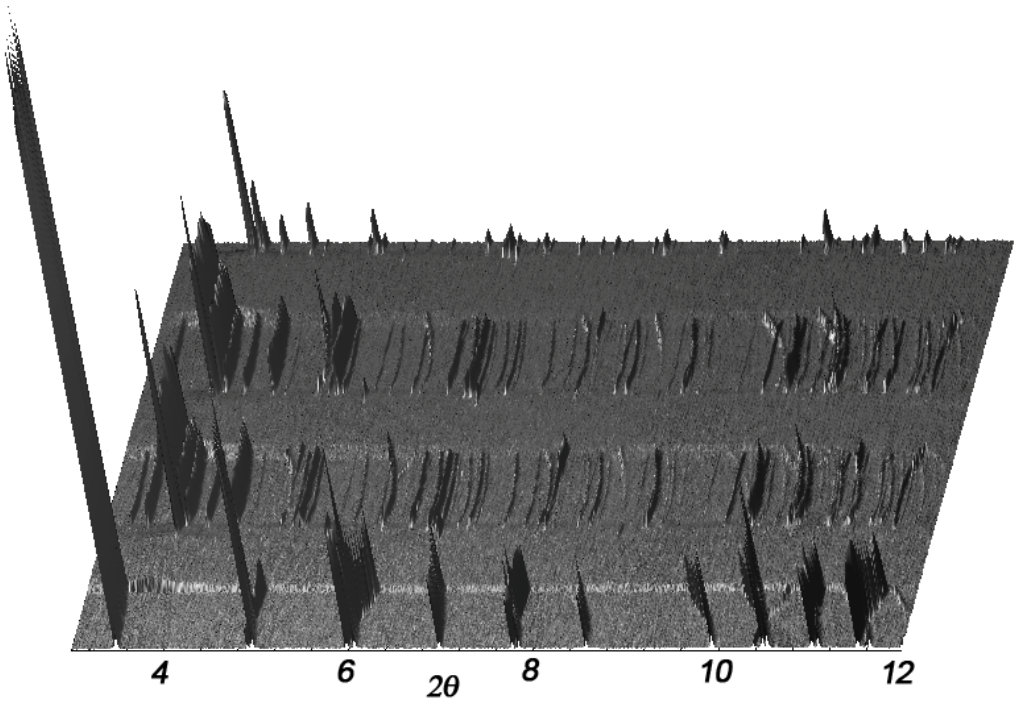

Fig. S9 The 3D plot of the X-ray powder diffractograms of $(N_{4444})_3[Pr(dcnm)_6]$ upon repeated heating and cooling at 5 K/min.

Table S2 The change in the unit cell parameters of $(N_{4444})_3[Pr(dcnm)_6]$ with an increase in temperature.

Temperature (K) [a]	*a* and *b* axes length (Å)	*c* axis length (Å)	Unit cell volume (Å^3)
273	17.8437(1)	22.2154(1)	6125.6(1)
291	17.9107(1)	22.1731(2)	6160.0(1)
309	18.0350(1)	22.0732(2)	6217.6(1)
330	18.2491(2)	21.8805(3)	6310.6(2)
350	18.5561(2)	21.6303(2)	6450.1(2)

a The temperature recorded at the commencement of the collection of the PXRD pattern.

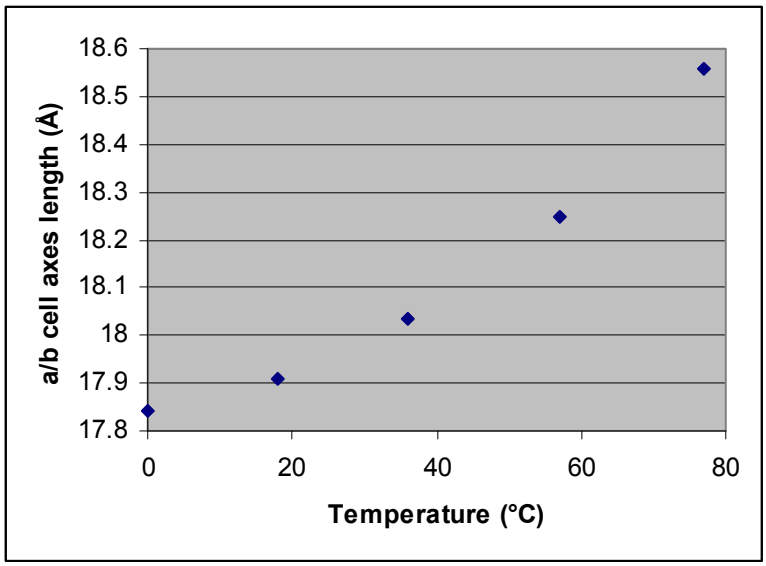

Fig. S10 The expansion of the *a* and *b* axes of the unit cell of $(N_{4444})_3[Pr(dcnm)_6]$ upon heating.

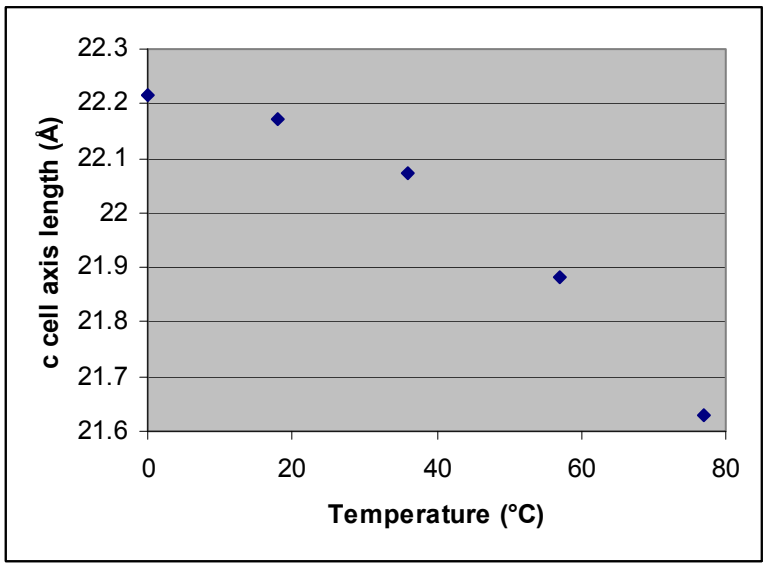

Fig. S11 The contraction of the *c* axis of the unit cell of $(N_{4444})_3[Pr(dcnm)_6]$ upon heating.

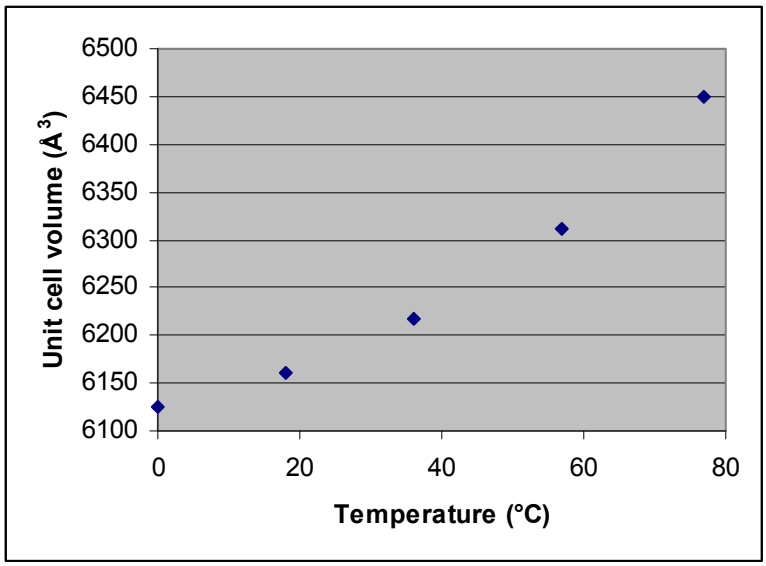

Fig. S12 The expansion of the unit cell of $(N_{4444})_3[Pr(dcnm)_6]$ upon heating.

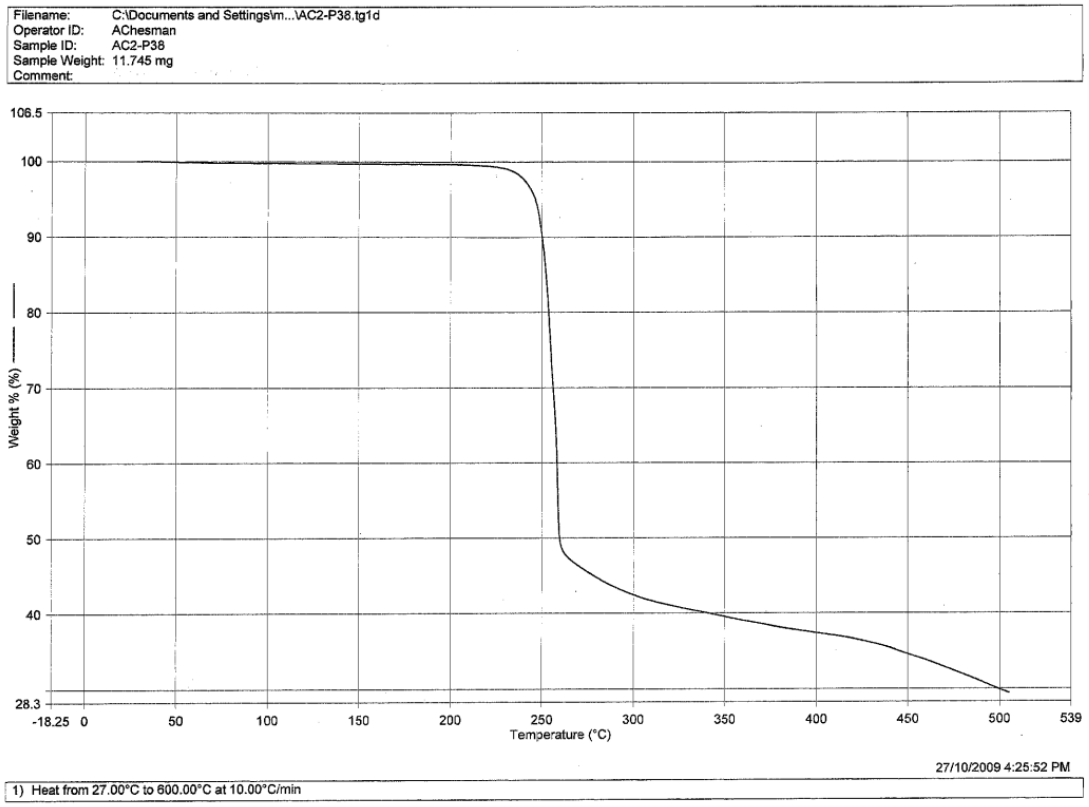

Fig. S13 Thermogram of $(N_{4444})_3[La(dcnm)_6]$.

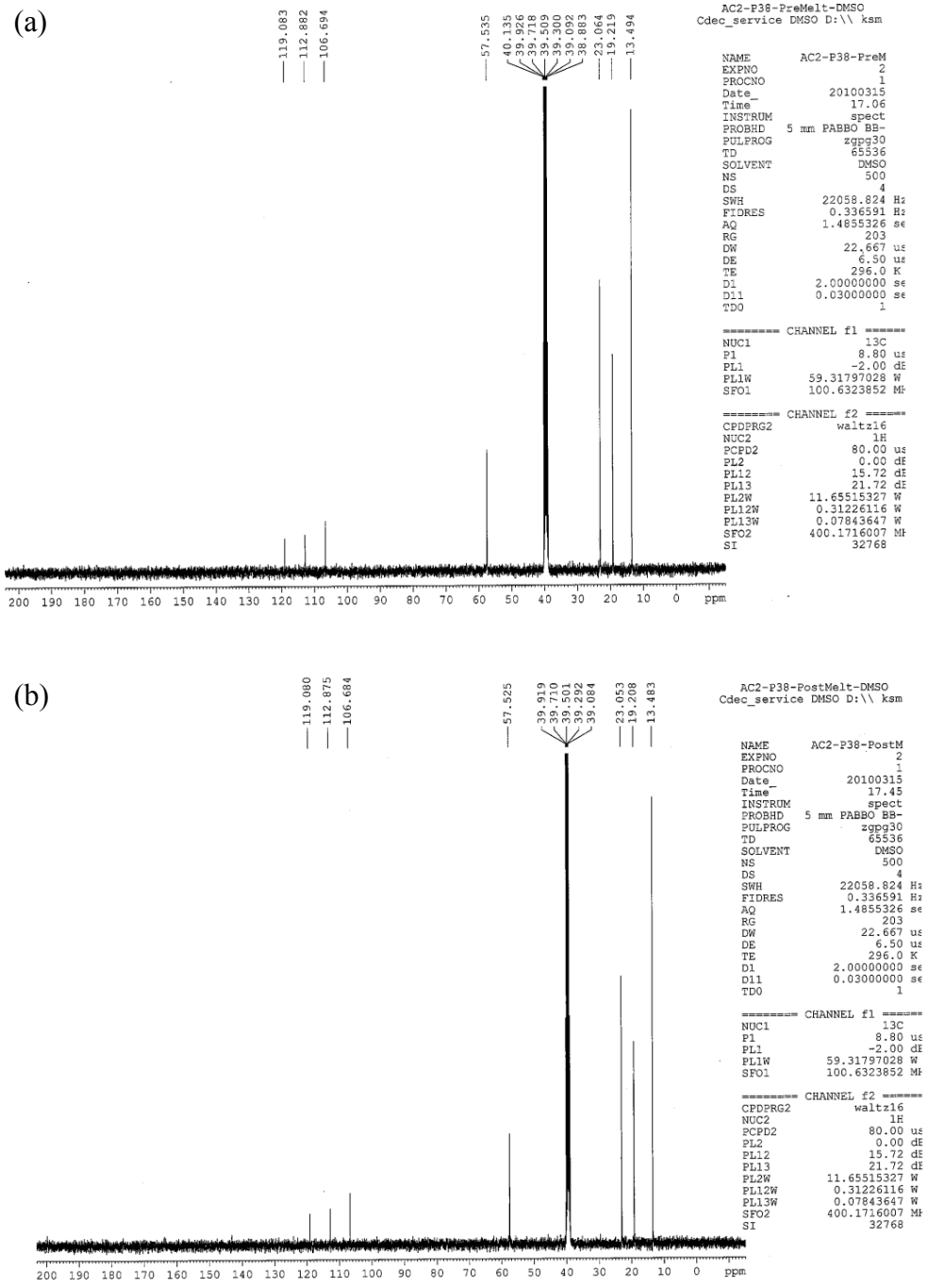

Fig. S14 ^{13}C NMR spectra of $(N_{4444})_3[La(dcnm)_6]$ (a) as synthesised and (b) recrystallised from a melt.

References

1. G. Longo, *Gazz. Chim. Ital.*, 1931, **61**, 575.

2. K. S. Wallwork, B. J. Kennedy, D. Wang, AIP Conference Proceedings, 2007, **879**, 879.

3. *Apex2*, v2.0, **2005**, Bruker AXS Ltd, Madison (WI), US

4. G. M. Sheldrick, *Acta Cryst.*, 2008, **A64**, 112.

5. L. J. Barbour, *J. Supramol. Chem.*, 2001, **1**, 189.

6. H. D. Flack, *Acta Cryst*., 1983, **A39**, 876.

7. Hunter, B. A.; Howard, C. J *LHPM-Rietica: a Computer program for Rietveld Analysis of X-ray and Neutron Powder Diffraction Patterns: User's Manual,* Australian Nuclear Science and Technology Organization Lucas Heights Research Laboratories, Menai, Australia, 2000.

8. C. F. Macrae, P. R. Edgington, P. McCabe, E. Pidcock, G. P. Shields, R. Taylor, M. Towler, J. van de Streek, *J. Appl. Cryst.*, 2006, **39**, 453.